IEEE Access
Multidisciplinary ⋮ Rapid Review ⋮ Open Access Journal

Received September 16, 2019, accepted October 12, 2019, date of publication October 22, 2019,
date of current version November 12, 2019.

Digital Object Identifier 10.1109/ACCESS.2019.2948938

Slant-Path Building Entry Loss at 24 Ghz

SAURAV DAHAL[1], (Student Member, IEEE), SHABBIR AHMED[1], (Member, IEEE), HORACE KING[1], (Senior Member, IEEE), GANESH BHARATULA[2], JOHN CAMPBELL[2], (Member, IEEE), AND MICHAEL FAULKNER[1], (Member, IEEE)

[1]Institute for Sustainable Industries and Liveable Cities, Victoria University, Melbourne, VIC 3011, Australia
[2]Telstra Corp Ltd., Melbourne, VIC 3000, Australia

Corresponding author: Saurav Dahal (saurav.dahal@live.vu.edu.au)

This research was supported by Telstra Corp Ltd.

ABSTRACT Results from an outdoor to indoor (O2I) measurement campaign emulating the satellite to indoor propagation channel at millimetre wave frequencies are presented in this paper. A link between a transmitter at a high altitude and a receiver placed at several locations on different floors of a building provided different slant path angles from the transmitter. The indoor receiver uses directional antennas with full spherical scanning capability which allows the measurement of signal strength as a function of antenna pointing direction, thus providing localized angle of arrival (AoA) information. Two directional horn antennas with different beamwidths are used for the indoor receiver. This allows the modelling of equipment incorporating adaptive beamforming. We synthesise the isotropic (0 dBi) antenna performance to enable comparison with the recent ITU (International Telecommunications Union) model. We observed that the mean building entry loss (BEL) increases by 0.43 dB per degree of slant elevation angle, almost twice the ITU recommendation. The signal decay with distance into the building had path loss slopes varying between 1.9 dB/m for a slant angle of 34° and 3.4 dB/m for a slant angle of 51°. We show that high gain narrow beam antennas outperform lower gain wider beamwidth antennas for reception (signal maximisation), but the performance improvement is significantly less than the gain difference between the two antennas. In terms of coexistence (interference minimisation), random alignment of the beam direction modestly enhances building entry loss (≈6 dB to 9 dB) which, after a certain limit, changes little with antenna gain.

INDEX TERMS Beamforming, building entry loss, indoor coverage, millimeter wave, penetration loss, satellite co-existence, slant angle.

I. INTRODUCTION

Millimetre waves (mmWave) enable an order of magnitude increase in bandwidth to greater than 1 GHz, but are subject to higher attenuation due to number of factors such as scattering, diffraction and building penetration. High Altitude Platforms (HAPs) want good indoor coverage whereas satellites want to restrict indoor coverage due to potential interference from mobile terminals into the satellite uplink channels. Building Entry Loss (BEL) is a parameter which determines the additional loss beyond that expected from just outside the building structure [1]. BEL measurements have been reported for frequencies below 6 GHz [2]–[6] but less have been reported for frequencies above 6 GHz [2], [7], [8]. A compilation of empirical data on BEL from different authors in different countries is available in [2], but only three out of the thirteen compiled mmWave measurements included slant angle of arrivals (one of which is a sub-set of the measurements presented here). Standardized models from organisations such as Third Generation Partnership Project (3GPP) provide only 0 dBi isotropic path loss characteristics as functions of distance and frequency [9]. However, directional beamforming is normally required for reliable mmWave links, therefore the isotropic characteristics may be less informative for the design and evaluation of systems employing directional antennas (or beamforming). Authors in [10]–[12] investigated the effect of antenna beamwidth on the BEL at 28, 32 and 38 GHz and found BEL increases as the beamwidth narrows. However, these were based on transmitter (Tx) and receiver (Rx) antennas at the same height. A ray tracing study has been done to study the BEL for a single slant path in [13]. To the best of our knowledge, there are very few reported BEL measurements that include mmWaves, directional antennas, slant path and full spherical

The associate editor coordinating the review of this manuscript and approving it for publication was Chow-Yen-Desmond Sim.

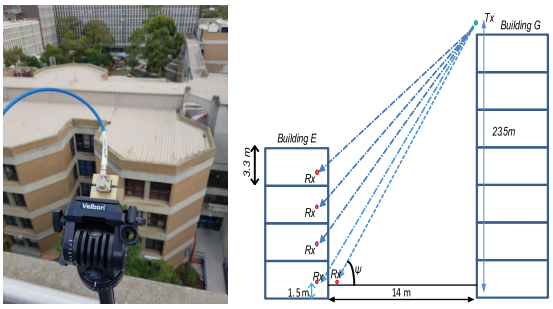

FIGURE 1. Building E from the Tx site on building G.

scanning over all azimuth and elevation angles ($0° > \phi > 360°$, $-90° > \theta > +90°$).

For frequencies below 6 GHz, the ITU-R Report M.2135 [14] reported a linear increase in path loss with internal distance, d, from the illuminated external wall, with a path loss slope of $m = 0.5$ dB/m. Authors in [7] studied the variation of BEL with in-building depth for 24 to 31 GHz and indicated that the increase in the path loss with internal distance at these frequencies could be higher than the $m * d$ suggested by the ITU-R Report M.2135. Other researchers measured m values between 0.2 dB/m and 1.0 dB/m for upward looking (i.e. transmitter on the ground) elevation angles between 0° to 30° [15], indicating a large variability when operating at mmWave frequencies. Here we report measurements for downward looking (elevated transmitter see Fig.1) slant angles (ψ) of over 30° and show even greater m values.

Recently a model for BEL has been developed by ITU for frequencies up to 100 GHz given by a combination of two log-normal distributions, based upon the frequency and the slant angle as:

$$L_{BE}(P) = 10\ log(10^{0.1A(P)} + 10^{0.1B(P)} + 10^{0.1C})\ dB \qquad (1)$$

where $L_{BE}(P)$ is the BEL not exceeded for probability P, and other variables defined as in the Appendix [16], [17]. The model specifies isotropic antennas, has a single median loss term and is not a function of d; the depth into the building being incorporated into the distribution itself. We compare our mmWave BEL measurements with this model.

We present results from a measurement campaign on slant-path building entry loss in the K/Ka bands around 24 GHz. We calibrated out the errors wherever possible, but some were out of our control such as human movement and small changes in environment between the two receive horn antenna measurement campaigns. Previous experience has shown that these differences average out in terms of macro parameters which are based on many measurements.

The signal received from a high rooftop transmitter into different floors of an adjacent building was used to determine path loss variation with slant angle, ψ. This enables the assessment of a) the unwanted signal leakage from transmitters within a building into a satellite's uplink channel for co-existence purposes and b) the desired signal in-building coverage from a high altitude platform (HAP) such as a drone or a balloon. The two use cases are identical when isotropic antennas are used for the indoor unit, but this changes when directional antennas are used. Indoor units employing adaptive antennas will adjust differently depending on whether the incoming signal is desired or not. Phase array antennas will be incorporated into future 5G user equipment to overcome increase path loss at mmWave frequencies. Thus, it is necessary to study how adaptive beamforming affects the building entry loss. We derive from our measurements the behaviour of a phase array antenna having the same beamwidths (gains) of our horn. Measurements were performed using two horn antennas of gain 9.6 dBi and 23.5 dBi from the same locations to identify how gain affects the results. The two antennas broadly model what can be expected from a user equipment (UE) with a 4 patch array (6 dB array factor + 5 dBi patch = 11 dBi) (approximately similar to 9.6 dBi gain horn) or a customer premises equipment (CPE) with a 64 patch array (18 dB array factor + 5 dBi patch = 23 dBi) (approximately similar to 23.5 dBi horn). In addition, we synthesise the isotropic antenna performance on which most channel models are based [16].

II. MEASUREMENT APPROACH

The measurement campaign was undertaken on the campus of Victoria University in Melbourne, Australia. The target building comprised of steel-reinforced concrete for structure and floors, with double-brick infill for external walls and a mix of double-brick and stud-and-plaster internal walls, topped by a near-flat zinc-coated ribbed-steel roof. The windows are single-glazed and set into aluminium frames. The lower 25% of the windows are reinforced with internal wire mesh. The general structural situation of building E under test is shown in Fig. 1, including the two transmitting antennas (Tx2 shown only) on top of building G. The building can generally be considered as 'traditional masonry construction' with minimal thermal efficiency measures.

The transmit horn antennas illuminated two of the target building's tower sections and were down-tilted and adjusted for bore-sight illumination of the particular target floor (Fig. 2). Each floor provides a certain slant-angle of incidence. Both antennas transmitted a 24 GHz continuous-wave (CW) signal. A small frequency offset of 2 MHz between the two trransmitted signals was used to identify each transmission.

The 'mobile' receiver (Rx) consisted of a calibrated standard horn antenna, placed on a rotating table, fed into a swept-frequency spectrum analyser; thus allowing concurrent measurements of the two slightly offset transmitted frequencies. The first set of slant path measurements was taken with the narrow half power beamwidth (HPBW) antenna (±5°, 23.5 dBi gain, here termed as 'narrow beam' (NB)). The azimuth (ϕ) coverage was in 7°steps over 360°, but the antenna size mechanically restricted the vertical coverage (θ) to seven steps of 10°, covering elevations between -25° to +45° [19], which in normal circumstances is more than enough to capture all received multipaths [13], [20]. However,

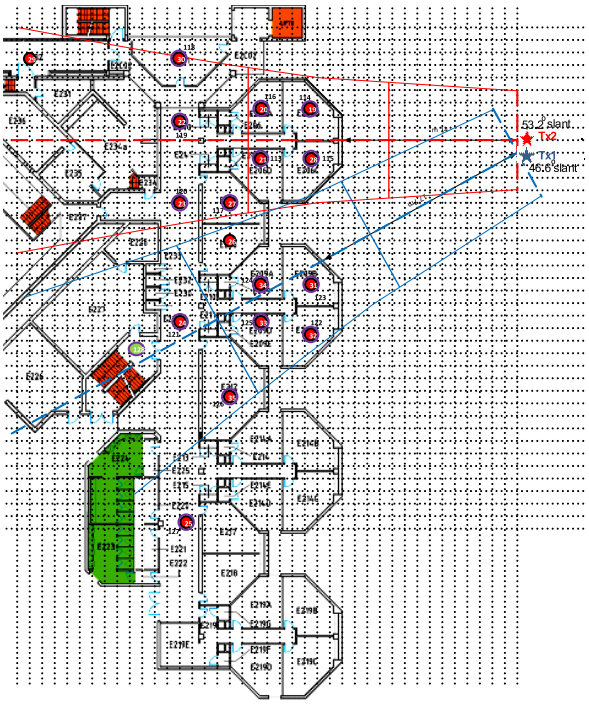

FIGURE 2. Receiver locations at level 2 of target building E. We replicate the positions on each floor as far as practically possible. Red and blue lines show the location within the HPBW of the transmit antenna. Receiver locations at level 1 in [18].

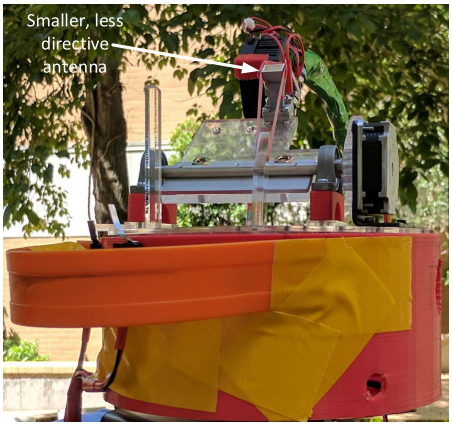

FIGURE 3. Modified receiver with 9.6 dBi antenna.

since we are dealing with signals from high altitude platforms, some multipaths could be missed. The measurements were repeated from the same locations with a smaller, but less directive antenna of ±23° HPBW (9.6 dBi, here termed as 'wide beam' (WB)), enabling expanded θ coverage between +83° and -83° from four pointing elevations of +60°, +20°, −20°, −60° (Fig. 3), giving close to full spherical coverage. In both cases the measurements are oversampled in the azimuth angle, ϕ, enabling interpolation down to 1°, but are close to critically sampled in the elevation angle θ making interpolation difficult.

For each orientation of the receiver horn (θ, ϕ), the spectrum analyser made 10 sweeps and recorded the average received power over these sweeps, and this process repeated

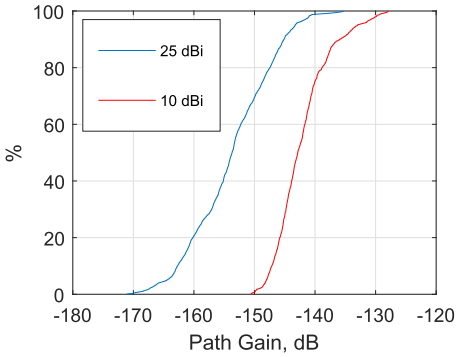

FIGURE 4. CDF of $PG(\theta, \phi)$ over all θ and ϕ measurement angles at position 2.

3 times. The received power $P(\theta, \phi)$ was used to obtain the mean path gain $PG(\theta, \phi)$ by removing the Tx Effective Isotropic Radiated Power (EIRP) and the Rx antenna gain, $G_{Rx}(boresight)$.

As an example, Fig. 4 shows the CDF (cumulative distribution function) of the directional dependent path gain $(PG(\theta, \phi))$ at position 2 (level 1) directly below position 20 on level 2 (Fig. 2) over all antenna pointing directions from the NB (23.5 dBi) and the WB (9.6 dBi) antenna. As $PG(\theta, \phi)$ is based on the *normalised* antenna radiation patterns ($G_{Rx}(boresight) = 0$ dBi) and does not include the Rx antenna gain, the NB antenna has lower $PG(\theta, \phi)$ compared to the WB antenna, since it is capturing less signal. The angular averaging effect of the WB antenna is evident in the reduced null depth and reduced dynamic range of the RHS (red) trace.

The signal level just outside the building is necessary as a reference for the BEL calculations, and is calculated from the free space path loss based on the 3D link distance from the transmitter (Fig. 2). Ground level measurements were used as a check and agreed within 0.5 dB of the calculated free space path loss (FSPL).

III. RESULTS

For each measurement location and each antenna we extracted the peak path gain (PG_{peak}) and reconstructed the isotropic (or omni) path gain (PG_{iso}) from the measured signals as follows [18], [21], [22].

For PG_{peak}, the path gain from the strongest direction is taken i.e. $PG_{peak} = max(PG(\theta, \phi))$, where $PG(\theta, \phi)$ is the path gain measured by the Rx antenna aperture. For PG_{iso}, we first sampled the polar path gain pattern in angular steps of HPBW in both azimuth and elevation, weighting each measurement to account for the lower arc as elevation increases and then sum i.e. $PG_{iso} = \sum\sum PG(\theta_i, \phi_j)cos(\theta_i)$, where azimuth $\phi_j = 0° : HPBW : 360°$ and elevation $\theta_i = -90° : HPBW : 90°$. In theory, both antennas should give the same 'isotropic' result for the same location, but in practice there is some variance since the measurements were not taken concurrently, and there was a bias due to the mechanically constrained elevation search angles, θ_i particularly for the NB antenna. Synthesis based on the WB antenna would

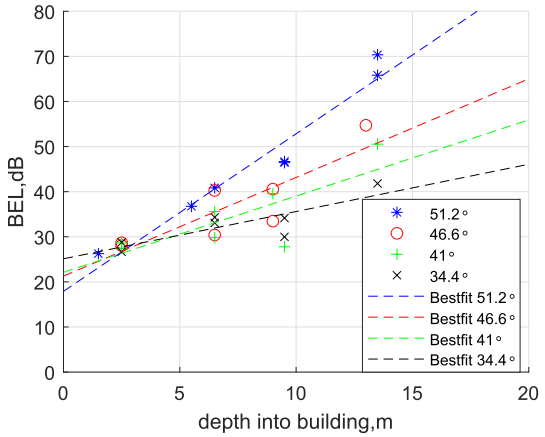

FIGURE 5. Isotropic BEL vs depth based on NB antenna for Tx1.

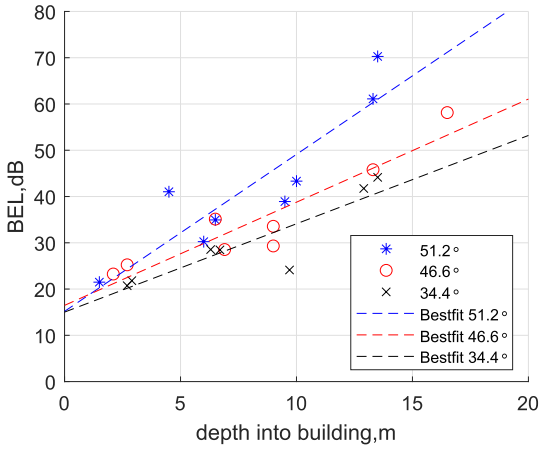

FIGURE 6. Isotropic BEL vs depth based on WB antenna for Tx1.

therefore give the closest isotropic approximation. Next we discuss BEL based upon these extracted PGs.

BEL WITH ISOTROPIC ANTENNAS

Building Entry Loss (BEL) (L_{BE}) is the difference between the measured PGs and the reference free space path gain (FSPG) obtained outside the illuminated face of the building structure [1];

$$L_{BE_{xxx}} = FSPG - PG_{yyy} \tag{2}$$

Thus BEL ($L_{BE_{xxx}}$) can be "minimum" ($L_{BE_{min}}$) or "isotropic" ($L_{BE_{iso}}$) or "directional" ($L_{BE}(\theta, \phi)$), corresponding to which path gain PG_{yyy} is used, PG_{peak}, PG_{iso} or $PG(\theta, \phi)$ respectively. BEL increases with depth into the building and is usually modelled by a linear dB variation with building depth (eq. 3)

$$L_{BE_{iso}}(d)\ [dB] = c + m\ d \tag{3}$$

where, d and m have been defined previously and c represents the loss through the building's outer wall measured at the facing wall's internal edge ($d = 0$). However the odd shape of the construction, with different angled faces and multiple entry points (windows) at different depths into the building made c more of an aggregate quantity. Therefore c was obtained along with m in a minimum mean square error (MMSE) estimate of the 'line-of-best-fit'. We also explored a power law variation based on the AB model [23]. In all cases, the linear model gave at least a 1 dB closer fit than the AB model for our measurements.

Fig. 5 and Fig. 6 show the scatter plot of the isotropic BEL ($L_{BE_{iso}}$) with building depth into the south tower from Tx1 for different slant angles (ψ) corresponding to each floor level. Generally, BEL increases with increased slant angle and this applies to both measurement antennas. As expected, the BEL increases as the measurement locations recede deeper inside the building and the variance increases, suggesting the existence of a complex multipath environment within the building. The 'line of best fit' for each floor shows the expected steeper slope (increase in m) with increase in

TABLE 1. BEL parameters with WB and NB antenna for Tx1.

Lvl	slant ψ	Bestfit (Isotropic)					
		σ (dB)		m		c (dB)	
		WB	NB	WB	NB	WB	NB
1	51.2	6.5	3.4	3.4	3.4	15.2	17.9
2	46.6	4.0	4.4	2.2	2.2	16.5	21.3
3	41.0	-	4.9	-	1.7	-	22.1
4	34.4	3.9	2.5	1.9	1.1	15.0	25.1

TABLE 2. Mean BEL with WB and NB antenna.

Lvl	Slant ψ	Tx1				Slant ψ	Tx2			
		$\overline{L_{BE_{min}}}$		$\overline{L_{BE_{iso}}}$			$\overline{L_{BE_{min}}}$		$\overline{L_{BE_{iso}}}$	
		WB	NB	WB	NB		WB	NB	WB	NB
1	51.2°	46.6	58.7	42.7	47.6	57.5°	43.7	55.2	40.6	44.8
2	46.6°	36.9	44.8	34.9	36.6	53.2°	41.2	53.6	38.1	43.7
3	41.0°	-	42.1	-	34.2	47.8°	37.9	46.1	34.4	37.9
4	34.4°	33.2	39.9	29.9	32.7	40.8°	37.2	43.5	33.8	34.9

slant angle, ψ, which is consistent with the more vertically orientated floor-ceiling reflections inside the building. Details of the 'line-of-best-fit' with, m, c are shown in Table 1 for Tx1 where σ is the standard deviation of the fit. Both NB and WB antennas have a similar path loss slope, $m = 3.4$ dB/m on level 1 ($\psi = 51.2°$), but this decreases to $m = 1.1$ and 1.9 for the NB and WB antennas respectively on level 4 ($\psi = 34.4°$). These figures are much higher than $m = 0.5$ dB/m for the M.2135 ITU model for <6 GHz [14] and the $0.7 \sin\psi$ variation in m for frequencies up to 38 GHz proposed by [15]. This is due to the higher slant angles under test and the internal walls and heavy clutter within the building. The effective loss through the buildings exterior wall (skin) $c \approx 15.3$ dB as measured by the WB antenna where as it is ≈21.5 dB as measured by the NB antenna. The latter measurement partially reflects the reduced signal collection from the mechanically constrained elevation angle, θ, of the NB measurement equipment.

The current ITU recommendation for BEL does not model the depth inside the building, relying instead on a single BEL distribution for each slant angle (ψ) [16]. The mean of the BEL measurements for each floor and from each transmitter are tabulated in Table 2 for both 'min' and 'isotropic' measurements. The mean is taken across all contributing

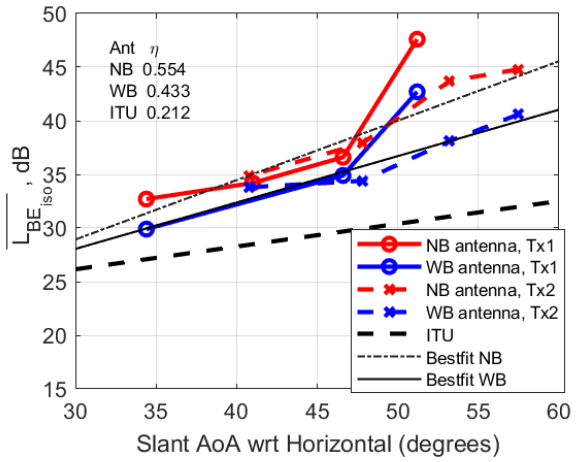

FIGURE 7. Mean Isotropic BEL ($\overline{L_{BE_{iso}}}$) vs slant angle for NB and WB antennas for Tx1 and Tx2.

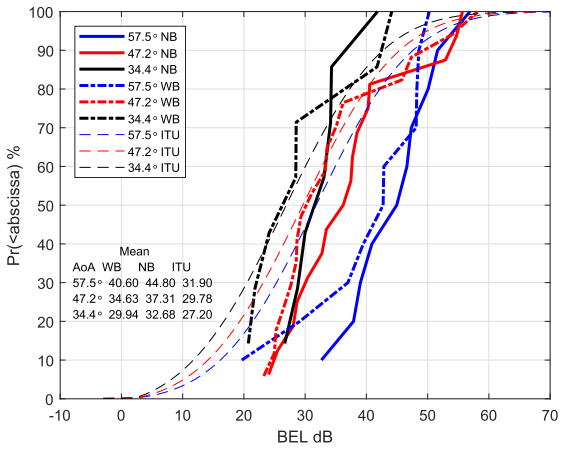

FIGURE 8. CDF of Isotropic BEL ($L_{BE_{iso}}$) with NB, WB and the ITU model at different slant angles.

locations in the Tx antennas HPBW for each slant angle ψ, as illustrated by Fig. 2 for floor level 2. The different geometries mean that Tx1 and Tx2 have different slant angle ψ values for the same floor level. Fig. 7 shows how the mean isotropic BEL ($\overline{L_{BE_{iso}}}$) values vary with ψ for each Tx. $\overline{L_{BE_{iso}}}$ increases with increasing slant angle, ψ. The restricted elevation coverage of the NB antenna shows up as a 1 dB to 5 dB additional path loss (compared to the WB antenna), particularly evident when ψ is over 50°. The abrupt increase in BEL from Tx1 at $\psi = 51.2°$ is due to tree clutter and a low iron roof partially shading the building's south tower ground floor (level 1) entrance. Leaving out this point a best fit line of all the remaining WB antenna based measurements (solid black) has a slope of $\eta = 0.433$ dB/degree of slant with a $\sigma = 0.77$ dB, which is a good fit. The slope is approximately twice the steepness of the ITU's recent model prediction of 0.212 dB/degree (shown as a black dashed line) for this type of building [16]. The mean BEL is closest to the ITU prediction at low slant angles, being within 3 dB for $\psi < 37°$.

Fig. 8 compares the ITU cdf of eq. 1 with the cdf of our isotropic BEL ($L_{BE_{iso}}$) measurements for three slant angles taking results from both Tx1 and Tx2 towers. It is not possible to compare the tails of the distributions as in [10] due to the limited number of measurements, however the average slope is not too dissimilar to the ITU recommendation. The WB antenna (dot-dashed line) closely aligns to the mid region of the ITU curves for $\psi = 34.4°$, but shifts to higher BEL at increased ψ. The higher loss of the NB antenna is clearly evident in the positive offset of the solid curves at low BEL (cdf$<$ 60%) when depth into the building is small. However this is not apparent for higher BEL's (cdf$>$ 60%) which would occur deeper into the building. Here, the NB and WB lines undergo a series of crossings indicating little signal is present outside the NB capture range ($|\theta| \approx> 45°$). Such signals have been reduced by reflection losses and scattering off internal objects converting the elevated signals into more horizontally propagating waves.

BEL WITH ADAPTIVE BEAMFORMING

In this section we include the effect of the receive antenna directivity and gain, G_{Rx}, to give the realistic antenna experience (rather than reconstruct the "isotropic" performance as per the previous section). This effectively removes the normalisation on Fig. 4. Including the directivity of the receive antenna is regarded as future work for the ITU standard [17].

The combined building entry loss (CBEL) measured at the receiver antenna port, $L_{BE,Grx}$, can be represented as a combination of loss due to building entry L_{BE} and gain due to receiver antenna G_{Rx} i.e.

$$L_{BE,Grx_{xxx}} = L_{BE_{xxx}} - G_{Rx} \tag{4}$$

For an isotropic Rx antenna, $G_{Rx} = 0$ dBi and $L_{BE_{iso}}$ of Fig. 7 equals $L_{BE,Grx_{iso}}$. With isotropic antennas BEL is the same whether it is being used to estimate the coverage from a high altitude platform or the co-existence with a high altitude platform. In the former the platform signal is desired, while in the latter case the platform signal is unwanted interference. This situation changes when adaptive beamforming is used, as in the case for mmWaves. Although, in all cases, the BEL is essentially the same, the effects of multiple entry points and the internal multipath environment combined with the antenna array pattern, gain and orientation makes for quite different receiver experiences. CBEL uses the same outside (0 dBi antenna) reference for comparing these different scenarios. When the high altitude platform forms the desired signal, the Rx array will beamsteer to the strongest direction, while in the co-existence case the array is focussed on signals from another basestation and so we assume the orientation is random with respect to the platform signal. Then, only occasionally will the beamsteered array coincide with the direction of max interference from the platform. We discuss these two situations next.

The lower 4 traces of Fig. 9 show the desired signal case when the Rx antenna is always beamformed to the direction of the strongest signal (minimum CBEL). Then $\overline{L_{BE,Grx_{min}}}$, the mean of the minimum combined entry loss from just

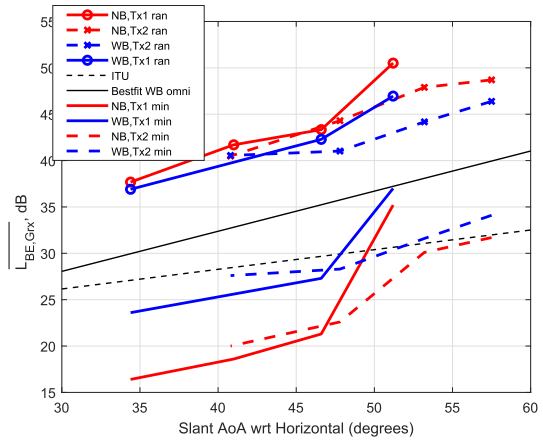

FIGURE 9. Mean directional CBEL ($\overline{L_{BE,Grx}(\theta,\phi)}$) and Mean minimum CBEL ($\overline{L_{BE,Grx_{min}}}$) vs slant angle for NB and WB antennas for Tx1 and Tx2.

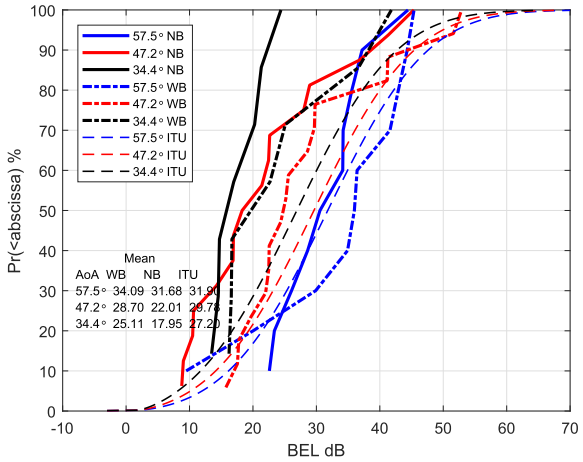

FIGURE 10. CDF of minimum CBEL ($L_{BE,Grx_{min}}$) with NB, WB and the ITU model at different slant angles.

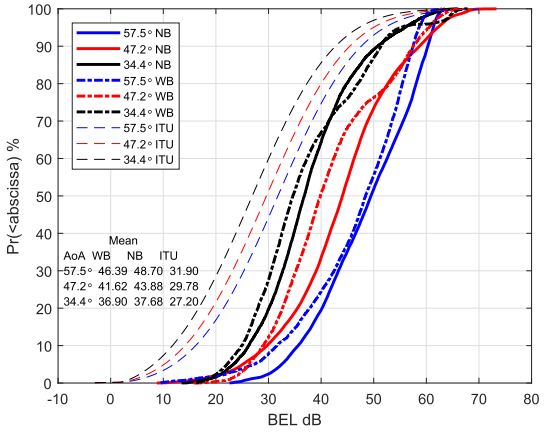

FIGURE 11. CDF of Directional CBEL ($L_{BE,Grx}(\theta,\phi)$) with NB, WB and the ITU model at different slant angles.

outside the building to the receiver's input port (which now includes the Rx antenna gain), is plotted against the slant angle, ψ. The WB antenna (blue) gives an average of ≈ 7 dB reduced CBEL than the isotropic best fit line (solid black) which is 2.6 dB short of the antennas 9.6 dBi gain. Similarly, comparing the NB antenna with the NB derived isotropic gives an average of $\approx$ 17.5 dB less CBEL which is 6 dB short of the 23.5 dBi gain of the antenna. The specified gain of the antennas is not fully realised because of the complex multiple direction of arrivals within the building [18], [24]–[26]. In this environment the gain reduction is 26% for both antennas. Also note that as the slant angles move from low ($\psi = 35°$) to high ($\psi > 50°$) the difference between the NB and WB antennas reduces from ≈ 7 dB to <3 dB caused by a fall in NB antenna gain as a growing proportion of signals from higher elevations are not being seen by the NB antenna. The cdf for three slant angles is shown in Fig. 10. Slopes are similar or slightly steeper than the ITU specified 0 dBi curves and the NB antenna outperforms the WB antenna in all except two locations, (characterised by low CBEL and a high slant angle).

The co-existence situation with random alignment is shown by the upper four traces in Fig. 9 (marked 'ran') where the mean is taken over all the measured angles from all locations contributing to the specified slant angle. Compared to the bestfit isotropic line we see a $\approx$7 dB increase in BEL for the WB antenna and $\approx$9 dB for the higher gain NB antenna (or $\approx$ 6 dB compared to the NB isotropic bestfit of Fig. 7). The increased CBEL is because the directive antenna's boresight is often pointing away from the incomming signals. Occasionally however the antenna will beamform into the minimum CBEL direction and the occurrence of this can be checked by the cdf of $\overline{L_{BE,Grx_{min}}}$, Fig. 11. Again we use the ITU cdf of eq. 1 as a reference. The higher number of measurement points gives a smoother curve with better rendition of the tails. The median value of CBEL is between 35 dB and 50 dB, but the tails go as low as 10 dB as they incorporate the wanted signal situation of Fig. 10 when the antenna is aligned for maximum response (minimum BEL). The cdf shows CBELs below 20 dB only occur with a probability of 2% for the most sensitive slant angle of $\psi = 34°$.

IV. CONCLUSION

Slant path BEL using directional antennas at mmWaves is important for both coverage and coexistence studies. BEL measurements at 24 GHz into an older style building are presented for different slant angles and different depths into the building, using 9.6 dBi and 23.5 dBi horn antennas for the indoor unit. The isotropic (0 dBi) performance is synthesised to allow comparisons to the recent ITU model. The signal loss into the building was best modelled as a linear increase in path loss (dB) with distance into the building. The slope increases with slant angle up to 3.4 dB/m; higher than previous published predictions [15]. The effective loss through the outside wall and windows was 15 dB. The variation of mean BEL with ψ is twice that suggested by the ITU indicating a much higher increased loss with slant angle for this building. The higher gain, NB antenna had a limited vertical scan angle that meant it could not see signals from above 45° or below -25° elevations. We use this fact to identify conditions where high elevation signals dominate, and this shows up at high

slant paths $\psi > 50°$ where the NB synthesised Isotropic BEL increased 5 dB compared to the WB synthesised Isotropic which had unrestricted scanning. Clearly the NB antenna misses the majority of the signal because the internal floor to ceiling reflections have elevation angles set by the incoming slant. The difference between NB and WB synthesised BEL measurements drops to ≈1 dB at $\psi = 30°$. Now, both NB and WB antennas give similar results.

Slant path BEL using beamformed antennas are not as yet covered by the ITU. We introduce the term CBEL, which combines BEL with the indoor antenna gain, to give a consistent outdside reference and then present measurements for two conditions, the desired signal condition and the co-existence condition. When the HAP is the desired signal source the CBEL is significantly reduced by beamforming, but not by the full antenna directivity gain as might be expected. Scattering within the building causes multiple AoAs which reduce the effective (dB) antenna gain by about 26% for both NB and WB antennas. In the co-existence case beamforming actually increases the CBEL compared to the Isotropic case, which is clearly a benefit and somewhat counter to the supposition in [17] indicating there would be no difference. However, the improvement is modest (in this case 6 dB to 9 dB dependent on slant angle) and limited by diminishing returns as the beamwidth is narrowed (1 dB to 3 dB further improvement going from WB to NB). We conclude that beamforming at mmWave frequencies is beneficial for slant path building entry in both coverage enhancement and co-existence with HAPs and satellites.

APPENDIX

The ITU parameters for building entry loss of equation (1) are given as [16]:

$$A(P) = F^{-1}(P)\sigma_1 + \mu_1 \tag{5}$$
$$B(P) = F^{-1}(P)\sigma_2 + \mu_2 \tag{6}$$
$$C = -3.0 \tag{7}$$
$$\mu_1 = L_h + L_e \tag{8}$$
$$\mu_2 = w + x\ log(f) \tag{9}$$
$$\sigma_1 = u + v\ log(f) \tag{10}$$
$$\sigma_2 = y + z\ log(f) \tag{11}$$
$$\tag{12}$$

where:

$$L_h = r + s\ log(f) + t\ (log(f))^2 \tag{13}$$

L_e is the correction for slant elevation angle, ψ:

$$L_e = 0.212\ |\psi| \tag{14}$$

f = frequency (GHz)
ψ = slant elevation angle (degrees)
P = probability that loss is not exceeded ($0 < P < 1$)
$F^{-1}(P)$ = inverse cumulative normal distribution as a function of probability.

For the traditional building, the coefficients are given as: $r = 12.64$, $s = 3.72$, $t = 0.96$, $u = 9.6$, $v = 2.0$, $w = 9.1$, $x = -3.0$, $y = 4.5$, $z = -2.0$

REFERENCES

[1] *Effects of Building Materials and Structures on Radiowave Propagation Above About 100 MHZ*,c document ITU-R, ITU-R P.2040-1, International Telecommunication Union, Report, 2015. [Online]. Available: https://www.itu.int/rec/R-REC-P.2040-1-201507-I/en

[2] *Compilation of Measurement Data Relating to Building Entry Loss*, document ITU-R 2346-2, International Telecommunication Union, 2017. [Online]. Available: https://www.itu.int/pub/R-REP-P.2346

[3] F. Perez-Fontan, V. Hovinen, M. Schönhuber, R. Prieto-Cerdeira, J. A. Delgado-Penín, F. Teschl, J. Kyrölänen, and P. Valtr, "Building entry loss and delay spread measurements on a simulated HAP-to-indoor link at S-band," *EURASIP J. Wireless Commun. Netw.*, vol. 2008, no. 11, pp. 11:1–11:6, Jan. 2008.

[4] T. Jost, G. Carrié, F. Pérez-Fontán, W. Wang, and U.-C. Fiebig, "A deterministic satellite-to-indoor entry loss model," *IEEE Trans. Antennas Propag.*, vol. 61, no. 4, pp. 2223–2230, Apr. 2013.

[5] D. I. Axiotis and M. E. Theologou, "An empirical model for predicting building penetration loss at 2 GHz for high elevation angles," *IEEE Antennas Wireless Propag. Lett.*, vol. 2, pp. 234–237, 2003.

[6] D. Axiotis and M. E. Theologou, "Building penetration loss at 2 GHz for mobile communications at high elevation angles by HAPS," in *Proc. 5th Int. Symp. Wireless Pers. Multimedia Commun.*, vol. 1, Oct. 2002, pp. 282–285.

[7] B. Guo, Y. Wu, J. Jiao, B. Lv, F. Zhou, Z. Ma, and J.-L. Sun, "Building entry loss model for 24 to 31GHz band," in *Proc. Int. Symp. Antennas Propag. (ISAP)*, Oct. 2016, pp. 60–61.

[8] C. R. Anderson, T. S. Rappaport, K. Bae, A. Verstak, N. Ramakrishnan, W. H. Tranter, C. A. Shaffer, and L. T. Watson, "In-building wideband multipath characteristics at 2.5 and 60 GHz," in *Proc. IEEE 56th Veh. Technol. Conf.*, vol. 1, Sep. 2002, pp. 97–101.

[9] *Study on Channel Model for Frequency Spectrum Above 6 GHZ Version 14.1.0.*, document 3GPP.38.900, Technical Specification, 3rd Generation Partnership Project, Jun. 2017.

[10] J. Lee, K.-W. Kim, M.-D. Kim, J.-J. Park, and H. K. Chung, "Empirical investigation of antenna beamwidth effects on the ITU-R building entry loss (BEL) model based on 32 GHz measurements," in *Proc. 11th Global Symp. Millim. Waves (GSMM)*, May 2018, pp. 1–3.

[11] J. Lee, M.-D. Kim, J.-J. Park, and Y. J. Chong, "Field-measurement-based received power analysis for directional beamforming millimeter-wave systems: Effects of beamwidth and beam misalignment," *ETRI J.*, vol. 40, no. 1, pp. 26–38, Feb. 2018.

[12] J. Lee, J. Liang, J.-J. Park, and M.-D. Kim, "Beamwidth-dependent directional propagation loss analysis based on 28 and 38 GHz urban microcellular (UMi) measurements," in *Proc. IEEE 86th Veh. Technol. Conf. (VTC-Fall)*, Sep. 2017, pp. 1–5.

[13] M. U. Sheikh, K. Hiltunen, and J. Lempiainen, "Enhanced outdoor to indoor propagation models and impact of different ray tracing approaches at higher frequencies," *Adv. Sci. Technol. Eng. Syst. J.*, vol. 3, no. 2, pp. 58–68, 2018.

[14] *Guidelines for Evaluation of Radio Interface Technologies for IMT-Advanced*, document ITU-R M.2135, ITU, 2008.

[15] M. Inomata, W. Yamada, M. Sasaki, and T. Onizawa, "Outdoor-to-indoor path loss model for 8 to 37 GHz band," in *Proc. Int. Symp. Antennas Propag. (ISAP)*, Nov. 2015, pp. 1–4.

[16] *Prediction of Building Entry Loss*, document ITU-R, ITU-R P.2109-0, International Telecommunication Union, Recommendation, 2017.

[17] R. Rudd, J. Medbo, F. Lewicki, F. S. Chaves, and I. Rodriguez, "The development of the new ITU-R model for building entry loss," in *Proc. 12th Eur. Conf. Antennas Propag. (EuCAP)*, Apr. 2018, pp. 1–5.

[18] S. Dahal, S. Ahmed, H. King, and M. Faulkner, "Antenna gain in a millimetre-wave multipath environment," in *Proc. Austral. Microw. Symp. (AMS)*, Feb. 2018, pp. 93–94.

[19] S. Dahal, M. Faulkner, H. King, and S. Ahmed, "27.1 GHz millimetre wave propagation measurements for 5G urban macro areas," in *Proc. IEEE 85th Veh. Technol. Conf. (VTC Spring)*, Jun. 2017, pp. 1–5.

[20] M. U. Sheikh, K. Hiltunen, and J. Lempiäinen, "Angular wall loss model and extended building penetration model for outdoor to indoor propagation," in *Proc. 13th Int. Wireless Commun. Mobile Comput. Conf. (IWCMC)*, Jun. 2017, pp. 1291–1296.

[21] S. Dahal, S. Ahmed, H. King, G. Bharatula, J. Campbell, and M. Faulkner, "Urban microcell 39 GHz measurements," *IEEE Antennas Wireless Propag. Lett.*, vol. 18, no. 10, pp. 2071–2075, Oct. 2019.
[22] S. Sun, G. R. MacCartney, M. Samimi, and T. S. Rappaport, "Synthesizing omnidirectional antenna patterns, received power and path loss from directional antennas for 5G millimeter-wave communications," in *Proc. IEEE Global Commun. Conf. (GLOBECOM)*, Dec. 2015, pp. 1–7.
[23] P. Kyosti, "Winner ii channel models," IST, Las Vegas, NV, USA, Tech. Rep. IST-4-027756 WINNER II D1.1.2V1.2, 2007.
[24] T. Taga, "Analysis for mean effective gain of mobile antennas in land mobile radio environments," *IEEE Trans. Veh. Technol.*, vol. 39, no. 2, pp. 117–131, May 1990.
[25] A. A. Glazunov, A. F. Molisch, and F. Tufvesson, "Mean effective gain of antennas in a wireless channel," *IET Microwaves, Antennas Propag.*, vol. 3, no. 2, pp. 214–227, Mar. 2009.
[26] A. A. Glazunov, "Theoretical analysis of mean effective gain of mobile terminal antennas in Ricean channels," in *Proc. IEEE 56th Veh. Technol. Conf.*, vol. 3, Sep. 2002, pp. 1796–1800.

SAURAV DAHAL received the bachelor's degree in electronics and communication engineering from Tribhuvan University, Kathmandu, Nepal, in 2011, and the master's degree in computer engineering with a major in wireless communication and networking from Chosun University, Gwangju, South Korea, in 2015. He is currently pursuing the Ph.D. degree in telecommunication with Victoria University, Melbourne, VIC, Australia. He received the Brain Korea 21 (BK 21) Plus Scholarship for studying master's degree in South Korea and is receiving the Victoria University Postgraduate Scholarship (VUPRS) for studying Ph.D. degree with Victoria University. His current research interests include networks and RF and millimeter wave systems.

SHABBIR AHMED received the Ph.D. degree from Victoria University, Melbourne, in 2013. His Ph.D. research involved the investigation of the major causes of interference that arise in co-locating base station transceivers. After his Ph.D. degree, he continued as a Research Fellow of wireless systems with the College of Engineering and Science, Victoria University, until 2017. He is currently a Senior EMC and RF Engineer with EMC Technologies, Melbourne. He is also a Lecturer with Victoria University. His current research interests include software radios, and RF and millimeter-wave systems.

HORACE KING received the degree from RMIT University, where he was with the research Centre for Advanced Technology in Telecommunication (CATT) doing research in Telecommunication and Teaching of Engineering Design Units for the third and fourth year Engineering streams after which he was with Swinburne and Monash. He is currently a Senior Lecturer in electrical engineering with the College of Engineering and Science, involved in teaching and coordinating telecommunication units at both undergraduate and postgraduate levels. He is also an active research member of Telecommunications, Electronics, Photonics and Sensors (TEPS) Research Centre. His current research interest includes telecommunication technologies, specifically in wireless communication of CDMA, LTE, and microwave and satellite communication systems.

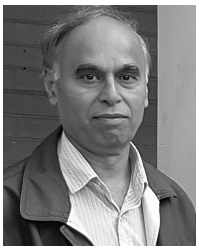

GANESH BHARATULA received the master's degree in microwave communications and electronics and another master's degree in solid state physics from Delhi University, India.

He was with the Tata Institute of Fundamental Research (India's premier research organization), developing microwave and satellite communication products for India's space research. He has been with Telstra Corporation Ltd., since 1984, starting first with IT Research Laboratories and then joining its CTO Department and Wireless Engineering. He is currently a Networks Principal with the Wireless Access Group and looks after assessment and development of emerging wireless technologies. Over the last 35 years, he has been providing technology leadership in regards to Telstra's current and future national and international mobile and fixed radio networks deployments in terms of standards influence, technology strategy, roadmap development, and performance assessment and tools. He has played key roles in Telstra's decisions to deploy 3G, 4G, and 5G.

He has authored several articles for reputed national and international journals and conferences.

JOHN CAMPBELL received the B.E. and M.Eng.Sc. degrees from The University of Melbourne. He started to work with Telstra (then Telecom Australia), in 1978. He was with Telstra's Research Laboratories, until 2006, then in their as a CTO, and Wireless Network Engineering Departments. He has recently retired from Telstra Corporation Ltd., where he was a Senior Wireless Technology Specialist. In his early years, he involved in pair cable, optical fiber, and high capacity digital radio systems after which his work focused on mobile wireless systems, involving the assessment of emerging wireless technologies and their impact on network capacity and performance, propagation measurements and modeling, network design tools, spectrum matters, and technology strategy. He presented the postgraduate subject wireless communication system at The University of Melbourne, from 1999 to 2016. His current research interests include physical layer technologies for 5G with focus on performance targets, coexistence, mm-wave systems, new waveforms, massive MIMO, 3GPP influence and the application of 5G to both mobile and fixed wireless access. He is currently involved with the Antennas and Propagation Society, Melbourne, Australia.

MICHAEL FAULKNER received the B.Sc. (Eng.) degree from the Queen Mary University of London, U.K., and the Ph.D. degree from the University of Technology, Sydney, Australia, in 1993. He is currently a Professor in telecommunications with Victoria University, Australia. His main research interest was in the application of (digital) signal processing techniques to the correction of the non-ideal characteristics of practical RF components; for example, quadrature modulators and power amplifiers. He has given tutorials, seminars, and invited articles on the above topic. Since then, his interests have broadened to encompass all physical layer aspects of wireless systems, with an emphasis on implementation. He has supervised research projects in radio propagation measurements (wideband channel sounding and direction of arrival), MIMO, transceiver algorithms, architectures and circuits, physical layer signal processing, and modulation. He has authored or coauthored over 100 publications and is regularly involved with industry sponsored research. His current research interests include wireless system design and fifth generation wireless technologies.